



Synthesis and characterisation of some water soluble ruthenium(II)–arene complexes and an investigation of their antibiotic and antiviral properties

Claire S. Allardyce^a, Paul J. Dyson^{a,*}, David J. Ellis^b, Paul A. Salter^a,
Rosario Scopelliti^a

^a Institut de Chimie Moléculaire et Biologique, Ecole polytechnique fédérale de Lausanne, Faculté des Sciences de Base, EPFL-BCH, CH-1015 Lausanne, Switzerland

^b Department of Chemistry, University of York, Heslington, York YO10 5DD, UK

Received 12 August 2002; received in revised form 22 September 2002; accepted 24 September 2002

Abstract

The water soluble ruthenium-*p*-cymene complexes $[\text{Ru}(\eta^6\text{-}p\text{-cymene})\text{X}_2]_2$ ($\text{X} = \text{Cl}, \text{Br}, \text{I}$ or NCS), $[\text{Ru}(\eta^6\text{-}p\text{-cymene})\text{X}_2(\text{pta})]$ ($\text{X} = \text{Cl}, \text{Br}, \text{I}$, or NCS ; $\text{pta} = 1,3,5\text{-triazza-7-phosphatricyclo}[3.3.1.1]\text{decane}$) and the tetraruthenium cluster $[\text{H}_4\text{Ru}_4(\eta^6\text{-}p\text{-benzene})_4]^{2+}$ have been prepared and their antimicrobial properties evaluated. They have been screened for antibacterial activity against *Escherichia coli*, *Bacillus subtilis*, *Pseudomonas aeruginosa*, for antifungal activity against *Candida albicans*, *Cladosporium resinae* and *Trichophyton mentagrophytes* and for antiviral activity against Herpes simplex and Polio viruses. The antimicrobial activity of these compounds does not appear to be correlated to DNA binding, but it could be due to specific interactions with proteins. The solid-state structure of the dimer complex $[\text{Ru}(\eta^6\text{-}p\text{-cymene})\text{Cl}_2]_2$, an important precursor complex in organometallic chemistry, is also reported.

© 2002 Elsevier Science B.V. All rights reserved.

Keywords: Ruthenium–arene complexes; Cluster; Bioorganometallic; Antimicrobial; Antibacterial; Antiviral; Anticancer

1. Introduction

The discovery of the anticancer drug cisplatin by Rosenberg in 1965 [1] (still used to treat around 70% of all cancer patients) led to considerable interest in metallopharmaceuticals that continues to this day. A large number of coordination compounds have been screened for anticancer and antimicrobial properties, but few are currently used in the clinic. One reason for failure in early clinical trials is due to the ligand exchange kinetics of coordination complexes resulting in a number of different species being present in solution. For entry into the clinic, each species must be isolated and characterised, which can prove challenging. Indeed, a ruthenium anti-metastatic drug Im-

$\text{H}[\text{Ru}(\text{Im})(\text{Me}_2\text{SO})\text{Cl}_4]$ (a more stable and reproducible solid) was developed from $\text{Na}[\text{Ru}(\text{Im})(\text{Me}_2\text{SO})\text{Cl}_4]$, which was not sufficiently stable in solution for clinical applications [2].

Organometallic compounds exhibit different ligand exchange kinetics in solution to coordination complexes, which could prove useful in drug design. The organometallic compounds that have been most widely studied for their medicinal properties are the metallocenes, $\text{M}(\eta^5\text{-C}_5\text{H}_5)_2\text{X}_2$. This group of compounds shows promising anticancer activity. The most active compounds are those where $\text{M} = \text{Ti}, \text{V}, \text{Nb}$ and Hf , moderate activity is observed for the Mo complex and Ta and W are essentially inactive [3]. The most successful of the metallocenes is $\text{Ti}(\eta^5\text{-C}_5\text{H}_5)_2\text{Cl}_2$, which is currently undergoing clinical trials [4]. Following the recent success of the ruthenium(III) anticancer drug $\text{ImH}[\text{Ru}(\text{Im})(\text{Me}_2\text{SO})\text{Cl}_4]$, which is currently in clinical trials at the Netherlands Cancer Institute of Amsterdam

* Corresponding author. Tel.: +41-21-6939854; fax: +41-21-6939885

E-mail address: paul.dyson@epfl.ch (P.J. Dyson).

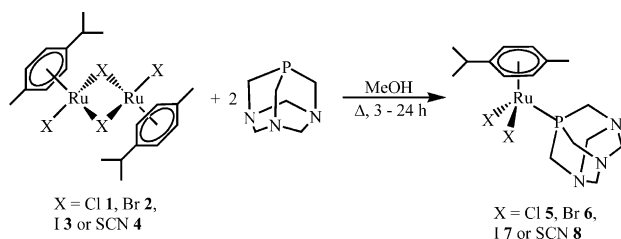
[5], the use of ruthenium(II)–arene complexes as potential anticancer agents has been explored. Ruthenium(II)–arene complexes were first shown to form adducts with nucleosides and nucleotides, forming mononuclear [6], di-, tri- and tetranuclear complexes [7]. Related compounds have also been evaluated as anticancer compounds [8] and the mechanisms of cytotoxicity have begun to be investigated [9].

Apart from applications as anticancer drugs, other medical applications of ruthenium compounds have been explored. Uses include immunosuppressants [10], nitric oxide scavengers [11] and antimicrobial agents [12]. It has been shown that ruthenium complexes of organic drugs can overcome resistance developed by the microbe to the organic compound alone. For example, a ruthenium(II)–chloroquine complex is two to fivefold more active than chloroquine against drug resistant *Plasmodium* parasites that cause malaria [13]. Similar results have been obtained when organic compounds that are used in the treatment of Chaga's disease and antibiotics such as thiosemicarbazone are derivatised with ruthenium [14]. In this paper we describe the selective antimicrobial and antiviral properties of a number of ruthenium(II)–arene compounds.

2. Results and discussion

The precursor compounds $[\text{Ru}(\eta^6\text{-}p\text{-cymene})\text{X}_2]_2$ ($\text{X} = \text{Cl}$ **1**, Br **2**, I **3** or NCS **4**) were made following literature protocols [15]. The pta derivatives of these compounds, viz. $[\text{Ru}(\eta^6\text{-}p\text{-cymene})\text{X}_2(\text{pta})]$ ($\text{X} = \text{Cl}$ **5**, Br **6**, I **7** or NCS **8**) were made from the dimer precursors by reaction with two equivalents of pta in methanol, at reflux, for 3–24 h (Scheme 1). This reaction, originally described by Zelonka for related species [15a], has been widely used to make compounds of this type [16]. The tetraruthenium–arene cluster $[\text{H}_4\text{Ru}_4(\eta^6\text{-benzene})_4]^{2+}$ (**9**), also derived from **1**, was made using a literature method [17]. Compounds **5–8** were characterised by electrospray ionisation mass spectrometry and $^{31}\text{P}\{^1\text{H}\}$ - and ^1H -NMR spectroscopy.

The positive ion electrospray ionisation mass spectra [18] of **5–8** exhibit similar features. Peaks corresponding to the parent ion with the addition of a proton, viz. $[\text{Ru}(\eta^6\text{-}p\text{-cymene})\text{X}_2(\text{pta})+\text{H}]^+$, are observed where X



Scheme 1.

coordinates relatively strongly to the ruthenium. Where the interaction is weaker, i.e. for **7** and **8**, ionisation is introduced by loss of one X-ligand, leading to the ion $[\text{Ru}(\eta^6\text{-}p\text{-cymene})\text{X}(\text{pta})]^+$.

The $^{31}\text{P}\{^1\text{H}\}$ - and ^1H -NMR spectra of compounds **5–8** are also similar and will be discussed together. Their $^{31}\text{P}\{^1\text{H}\}$ -NMR spectra in CDCl_3 consist of a singlet resonance in the region $\delta -30.29$ to -36.24 . The ^1H -NMR spectra of compounds **5–8** all show signals that can be attributed to the coordinated *p*-cymene ring and the pta ligand. A quartet between $\delta 5.34$ and 5.46 can be assigned to the aromatic ring protons of the *p*-cymene ligand. The most distinctive feature of the *p*-cymene ligand is the septet between $\delta 2.60$ and 2.90 , which is due to the single CH proton of the isopropyl group. The methyl group protons of the same group give rise to a doublet between $\delta 1.19$ and 1.22 . A singlet between $\delta 2.08$ and 2.90 can be assigned to the methyl group that is attached directly to the aromatic ring. The pta ligand gives rise to two singlet resonances. The one at higher frequency between $\delta 4.43$ and 4.53 may be assigned to the CH_2 protons in the nitrogen heterocycle and the one at lower frequency between $\delta 4.22$ and 4.36 corresponds to the CH_2 protons in the phosphorus–nitrogen heterocycle.

Compounds **1–4** are soluble in water and since water is a good nucleophile it is likely that the dimer is cleaved into monomer units upon dissolution to form $[\text{Ru}(\eta^6\text{-}p\text{-cymene})\text{Cl}_2(\text{H}_2\text{O})]$. However, we were unable to characterise this hypothetical water species by conventional means. Attempts to crystallise the water derivative resulted in crystallisation of **1**. Compound **1** has been used extensively as a starting material in organometallic chemistry and somewhat surprisingly its crystal structure has not been reported previously. Since it is such an important precursor its structure will be briefly described here. The structure of **1** (Fig. 1) contains 1.5

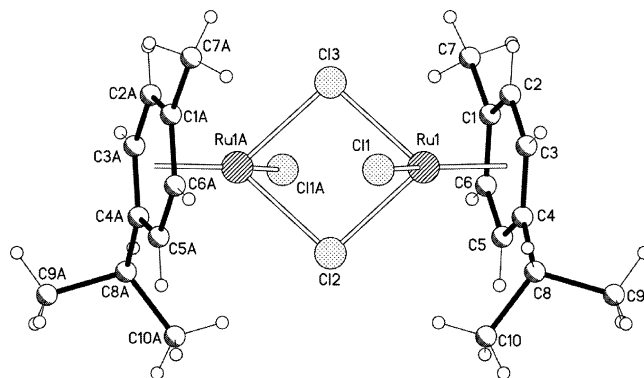


Fig. 1. A ball-and-stick representation of the crystal structure of **1** lying on the twofold axis. Letter A indicates the following symmetry transformation: $-x, -y, z$. Key bond lengths (Å) include: $\text{Ru}(1)\text{--C}(1)$ 2.153(7), $\text{Ru}(1)\text{--C}(2)$ 2.151(7), $\text{Ru}(1)\text{--C}(3)$ 2.153(6), $\text{Ru}(1)\text{--C}(4)$ 2.157(7), $\text{Ru}(1)\text{--C}(5)$ 2.159(7), $\text{Ru}(1)\text{--C}(6)$ 2.157(6), $\text{Ru}(1)\text{--Cl}(1)$ 2.416(3), $\text{Ru}(1)\text{--Cl}(2)$ 2.464(3), $\text{Ru}(1)\text{--Cl}(3)$ 2.451(3).

independent molecules that show some disorder problems. Structure refinement details are given in Section 3 and Table 1 lists the crystal data and refinement parameters. The independent molecule which does not lie on a twofold axis shows two different dispositions. As the occupancy factor calculated for site A is close to one it was not possible to obtain both dispositions except for the metal ions and for two of the four chlorines as shown in Fig. 2. Principal bond lengths for **1** are given in the caption to Fig. 1. Essentially, each ruthenium(II) centre possesses a distorted octahedral geometry composed of the *p*-cymene ring, one terminal and two bridging chlorines. The C₆-ring with an average Ru–C bond length of 2.15, 2.16 and 2.16 Å for the three unique ruthenium atoms. The bridging chlorine ligands lie in the range 2.252(10)–2.668(10) Å and the terminal chlorines 2.41(3)–2.45(3) Å, but caution should be applied into any interpretation of these distances due to the disorder present.

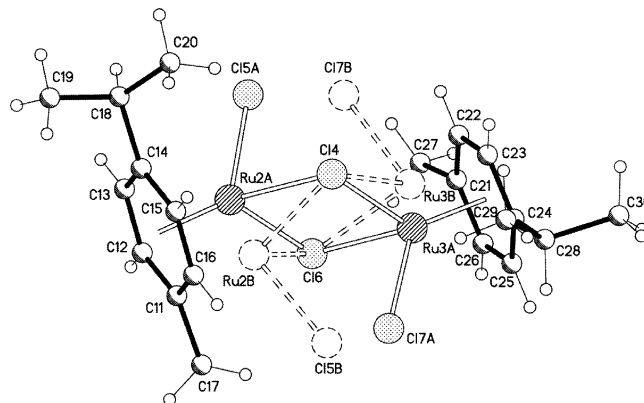


Fig. 2. A ball-and-stick representation of **1** showing the two different dispositions (named A and B) for the metal ions and two of the four chlorines. Key bond lengths (Å) include: Ru(2A)–C(11) 2.190(7), Ru(2A)–C(12) 2.174(7), Ru(2A)–C(13) 2.140(7), Ru(2A)–C(14) 2.122(7), Ru(2A)–C(15) 2.139(7), Ru(2A)–C(16) 2.172(6), Ru(2A)–Cl(4) 2.461(3), Ru(2A)–Cl(5A) 2.435(3), Ru(2A)–Cl(6) 2.488(3), Ru(3A)–C(21) 2.180(7), Ru(3A)–C(22) 2.176(7), Ru(3A)–C(23) 2.159(7), Ru(3A)–C(24) 2.146(7), Ru(3A)–C(25) 2.151(6), Ru(3A)–C(26) 2.168(7), Ru(3A)–Cl(4) 2.437(3), Ru(3A)–Cl(6) 2.450(3), Ru(3A)–Cl(7A) 2.420(3).

Table 1
Crystal data and structure refinement for **1**

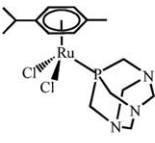
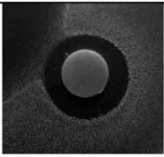
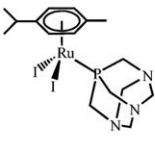
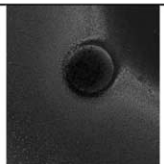
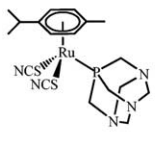
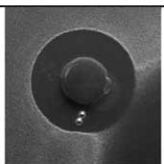
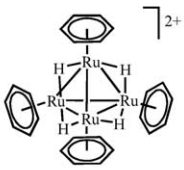
Empirical formula	C ₂₀ H ₂₈ Cl ₄ Ru ₂
Formula weight	612.36
Temperature (K)	140(2)
Wavelength (Å)	0.71073
Crystal system	Orthorhombic
Space group	<i>Fdd2</i>
Unit cell dimensions	
<i>a</i> (Å)	47.063(3)
<i>b</i> (Å)	15.6748(10)
<i>c</i> (Å)	18.8937(13)
α (°)	90
β (°)	90
γ (°)	90
<i>V</i> (Å ³)	13938.0(15)
<i>Z</i>	24
<i>D</i> _{calc} (Mg m ⁻³)	1.751
Absorption coefficient (mm ⁻¹)	1.763
<i>F</i> (000)	7296
Crystal size (mm ³)	0.34 × 0.22 × 0.18
Theta range for data collection	3.38–29.15°
Index ranges	–64 ≤ <i>h</i> ≤ 63, –17 ≤ <i>k</i> ≤ 21, –24 ≤ <i>l</i> ≤ 25
Reflections collected	26266
Independent reflections	8144 [<i>R</i> _{int} = 0.0775]
Completeness to theta = 29.15°	94.2%
Absorption correction	Empirical (DELABS)
Max/min transmission	0.775 and 0.360
Refinement method	Full-matrix least-squares on <i>F</i> ²
Data/restraints/parameters	8144/263/331
Absolute structure parameter	0.31(10)
Final <i>R</i> indices [<i>I</i> > 2σ(<i>I</i>)]	<i>R</i> ₁ = 0.0726, <i>wR</i> ₂ = 0.1946
<i>R</i> indices (all data)	<i>R</i> ₁ = 0.0971, <i>wR</i> ₂ = 0.2159
Goodness-of-fit on <i>F</i> ²	1.074
Largest difference peak and hole	2.521 and –1.183 (e Å ⁻³)

The pta derivatives **5–8** are soluble in polar organic solvents, alcohols, water and even ionic liquids. Solubility is determined (or even controlled) by the pta ligand. When the pta ligand is protonated these complexes are preferentially soluble in water and when deprotonated solubility in organic solvents is favoured. The structure of the pta derivative of **1**, i.e. **5** has been reported previously, and that of **6** has also been partially solved. This latter structure is disordered and also contains LiBr, with the lithium ion associated with the nitrogens on the pta ligand. The cluster **9** is highly soluble in ionic liquids [19] and water and its structure is known [20].

2.1. Antimicrobial activity

The cytotoxicity of compounds **1**, **2** and **5–9** was measured against six types of microbes (see Table 2). The microbes used were the bacteria *Escherichia coli*, *Bacillus subtilis*, *Pseudomonas aeruginosa* and the fungi *Candida albicans*, *Cladosporium resinae* and *Trichophyton mentagrophytes*. The dimers **1** and **2** and the cluster **9** were inactive, whereas the pta derivatives showed varying degrees of activity. This would suggest that the pta ligand plays a role in cytotoxicity. We have previously postulated that the pta group could facilitate the ability of a compound to cross a cell membrane. As mentioned above, pta+H⁺, is preferentially water soluble whereas pta is preferentially soluble in polar organic solvents. Cell membranes are quite hydrophobic otherwise the cell environment is largely aqueous. We have also observed that the lithium cation in the structure of **6** interacts with the pta ligand. It is possibly

Table 2
Antimicrobial activity of the compounds

Number	Compound	Antimicrobial activity	
		Strain	Activity
5		<i>C. resinae</i>	 (2 mm)
7		<i>B. subtilis</i>	
8		<i>T. mentagrophytes</i>	 (3 mm)
9		Polio	(2+ mm)

this dynamic property of the pta ligand that facilitates the uptake mechanism.

There is also a correlation of the activity of $[\text{Ru}(\eta^6\text{-}p\text{-cymene})\text{X}_2(\text{pta})]$ **5–8** with the type of X-ligands present. The chloride derivative **5** inhibited the growth of *T. mentagrophytes* and the NCS derivative **8** inhibited the growth of *C. resinae*. In contrast, the iodide derivative **7** slightly retarded the growth of *B. subtilis*, but this microbe is the most sensitive to non-specific cytotoxicity and the effect is likely to be a result of the general toxicity of this compound, rather than specific inhibition of *B. subtilis*. Although this is a relatively small study, using a limited number of microbes and compounds, the results demonstrate how the specificity of antimicrobial activity can be altered by the ligands attached to the ruthenium centre.

The mechanism of antimicrobial activity of the pta complexes does not appear to be correlated to the general toxicity of the compounds. In addition, cytotoxicity does not appear to be correlated to the DNA damaging activity of these compounds. The gel shift assays in Fig. 3 show that compounds **5** and **6** induce more DNA damage than the other compounds in the

series, and would therefore be predicted to be the most toxic compounds if DNA damage was a major contributor to toxicity. This is in accordance with other reports that suggest the biological activity of other ruthenium compounds involve specific protein targets [21].

To test this hypothesis *E. coli* cells were incubated with **5**, then the proteins were extracted and partially separated by non-reducing gel electrophoresis. The gel lanes were then analysed by laser ablation inductively coupled plasma mass spectrometry (ICP-MS) and the m/z of ruthenium was detected across the gel (see Fig. 4) that was not observed in the control. There would appear to be very specific protein–ruthenium interactions, which contrasts to that of cisplatin, which has also been analysed using this protocol [22].

2.2. Antiviral activity

Compounds **1**, **2** and **5–9** were also measured against the Herpes simplex and Polio viruses. No activity was detected for compounds **1**, **2** and **5–8**, whereas $[\text{H}_4\text{Ru}_4(\eta^6\text{-}p\text{-benzene})_4]^{2+}$ (**9**) was active against Polio

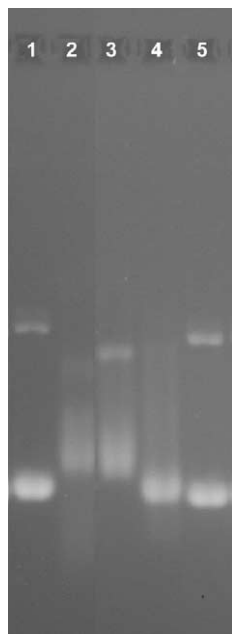


Fig. 3. DNA binding assays for compounds **5–8** in aqueous solution: Lane 1, DNA alone (control); Lane 2, compound **5**; Lane 3, compound **6**; Lane 4, compound **7**; Lane 5, compound **8**.

without inhibiting the growth of human cells, thus, its side effects could be minimal, despite the fact that this compound has previously been shown to damage DNA [23]. It is possible that **9** is cytotoxic only in Polio infected cells as the virus effects cell membrane permeability facilitating uptake of the cluster. In fact, the cluster was originally selected as a potential anticancer agent as it could selectively accumulate in cancer tissues based on the ‘enhanced permeability and retention’ effect that results in a dramatic increase in blood vessel permeability within diseased tissues compared to normal tissues [24].

2.3. Concluding remarks

Ruthenium complexes are of particular interest for clinical applications as they have similar ligand ex-

change kinetics as the successful and widely used platinum compounds. In addition, ruthenium compounds have low general toxicity, possibly through mimicking iron binding to biological molecules for transport and storage [25]. While ruthenium(III) compounds have been most widely studied to date, they are believed to be activated by reduction to ruthenium(II) in cancer cells prior to binding to DNA [26]. We have shown that a number of ruthenium(II)-*p*-cymene compounds have quite different antimicrobial and antiviral properties. None of the activities were due to general toxicity, rather specific activities were noted. For compounds $[\text{Ru}(\eta^6\text{-}p\text{-cymene})\text{X}_2(\text{pta})]$ **5–8** activity depended upon the type of ligand, X. In the next phase of our experiments we intend to see how specificity is effected by varying the arene ligand. In related compounds, it has been proposed that for DNA binding the ring initially intercalates and this is followed by covalent bonding between the ruthenium and the DNA [9]. The cluster **9** shows considerable promise, as it inhibits the growth of the Polio virus but does not effect the growth of human cells. We also intend to study the effects of varying the arene on biological function.

3. Experimental

3.1. Compound preparation

The dimers $[\text{Ru}(\eta^6\text{-}p\text{-cymene})\text{X}_2]_2$ (X = Cl **1**, Br **2**, I **3** or NCS **4**) [15] and the cluster $[\text{H}_4\text{Ru}_4(\eta^6\text{-benzene})_4]^{2+}$ (**9**) [20] were made following literature protocols. The new compounds described herein were made under an inert atmosphere using pre-dried solvents. All subsequent purification was carried out in air. Electrospray mass spectrometry was performed using a VG Autospec mass spectrometer. ^{31}P - and ^1H -NMR spectra were recorded on either a 270 MHz JEOL JNM-EX270 FT-NMR instrument or a 500 MHz Bruker AMX500 FT-NMR spectrometer. ^{31}P -NMR spectra were calibrated

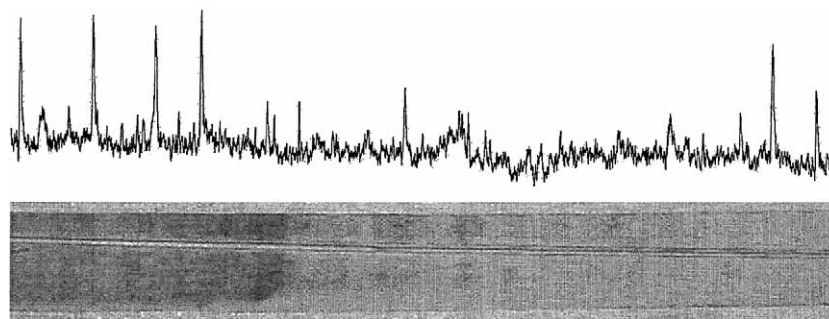


Fig. 4. Non-reducing polyacrylamide gel electrophoresis results for the separation of SDS-denatured proteins from whole bacterial cells after incubation with **5**; (top) the ICP-MS trace showing the amount of ruthenium as a percentage of the maximum reading (6.19×10^4 counts) with distance along the gel and (bottom) a photograph of the gel aligned with the ICP-MS trace.

to an internal phosphoric acid standard and ^1H spectra were calibrated using solvent peaks.

3.2. Synthesis of $\text{Ru}(\eta^6\text{-}p\text{-cymene})(\text{pta})\text{Cl}_2$ (**5**)

A solution of $[\text{Ru}(\eta^6\text{-}p\text{-cymene})\text{Cl}_2]_2$ (306 mg, 0.5 mmol) and pta (157 mg, 1.0 mmol) in MeOH (100 ml) was heated to reflux for 3 h during which time the initial orange–red solution became deep red in colour. Upon cooling, a small amount of black insoluble matter precipitated which was removed by filtration. Removal of the solvent under reduced pressure and further drying for 2 h on a vacuum line gave a deep red microcrystalline solid (438 mg, 0.946 mmol, 94%).

Spectroscopic data for **5**: ESMS (positive ion) m/z 428 $[\text{Ru}(\text{C}_{10}\text{H}_{14})(\text{pta})\text{Cl}_2]^+$; $^{31}\text{P}\{^1\text{H}\}$ -NMR (CDCl_3): -36.24 (s); ^1H -NMR (CDCl_3): 5.46 (q, $J = 6.57$ Hz, 4H), 4.53 (s, 6H), 4.32 (s, 6H), 2.78 (septet, $J = 6.89$ Hz, 1H), 2.08 (s, 3H), 1.22 (d, $J = 6.93$ Hz, 6H).

3.3. Synthesis of $\text{Ru}(\eta^6\text{-}p\text{-cymene})(\text{pta})\text{Br}_2$ (**6**)

A solution of $[\text{Ru}(\eta^6\text{-}p\text{-cymene})\text{Br}_2]_2$ (393 mg, 0.5 mmol) and pta (157 mg, 1.0 mmol) in MeOH (100 ml) was heated to reflux for 3 h during which the initial orange solution became deep red in colour. Upon cooling, the solution was filtered and removal of the solvent under reduced pressure and further drying for 2 h on a vacuum line gave a deep red microcrystalline solid (524 mg, 0.953 mmol, 95%).

Spectroscopic data for **6**: ESMS (positive ion) m/z 553 $[\text{Ru}(\text{C}_{10}\text{H}_{14})(\text{pta})\text{Br}_2 + \text{H}]^+$, 472 $[\text{Ru}(\text{C}_{10}\text{H}_{14})(\text{pta})\text{Br}]^+$; $^{31}\text{P}\{^1\text{H}\}$ -NMR (CDCl_3): -34.78 (s); ^1H -NMR (CDCl_3): 5.46 (q, $J = 5.74$ Hz, 4H), 4.53 (s, 6H), 4.36 (s, 6H), 2.90 (septet, $J = 6.67$ Hz, 1H), 2.90 (s, 3H), 1.21 (d, $J = 6.79$ Hz).

3.4. Synthesis of $\text{Ru}(\eta^6\text{-}p\text{-cymene})(\text{pta})\text{I}_2$ (**7**)

A solution of $[\text{Ru}(\eta^6\text{-}p\text{-cymene})\text{I}_2]_2$ (500 mg, 0.511 mmol) and pta (160 mg, 1.022 mmol) in MeOH (100 ml) was heated to reflux for 24 h during which the initial red/purple solution became deep purple in colour. Upon cooling, the solution was filtered and removal of the solvent under reduced pressure and further drying for 2 h on a vacuum line gave a purple microcrystalline solid (642 mg, 0.994 mmol, 97%).

Spectroscopic data for **7**: ESMS (positive ion) m/z 519 $[\text{Ru}(\text{C}_{10}\text{H}_{14})(\text{pta})\text{I}]^+$; $^{31}\text{P}\{^1\text{H}\}$ -NMR (CDCl_3): -35.02 (s); ^1H -NMR (CDCl_3): 5.42 (q, $J = 6.04$ Hz, 4H), 4.51 (s, 6H), 4.36 (s, 6H), 2.81 (septet, $J = 6.68$ Hz, 1H), 2.22 (s, 3H), 1.19 (d, $J = 6.64$ Hz).

3.5. Synthesis of $\text{Ru}(\eta^6\text{-}p\text{-cymene})(\text{pta})(\text{SCN})_2$ (**8**)

A solution of $[\text{Ru}(\eta^6\text{-}p\text{-cymene})(\text{SCN})_2]_2$ (450 mg, 0.641 mmol) and pta (201 mg, 1.282 mmol) in MeOH (100 ml) was heated to reflux for 5 h during which the initial yellow solution became bright red in colour. Upon cooling, the solution was filtered and removal of the solvent under reduced pressure and further drying for 2 h on a vacuum line gave a bright yellow/red microcrystalline solid (632 mg, 1.244 mmol, 97%).

Spectroscopic data for **8**: ESMS (positive ion) m/z 645 $[\text{Ru}_2(\text{C}_{10}\text{H}_{14})_2(\text{SCN})]^+$, 451 $[\text{Ru}(\text{C}_{10}\text{H}_{14})(\text{pta})(\text{SCN})]^+$; $^{31}\text{P}\{^1\text{H}\}$ -NMR (D_2): -30.29 (s); ^1H -NMR (CD_3OD) 5.34 (q, $J = 6.43$ Hz, 4H), 4.43 (s, 6H), 4.22 (s, 6H), 2.60 (septet, $J = 6.60$ Hz, 1H), 2.11 (s, 3H), 1.22 (d, $J = 6.61$ Hz).

3.6. Structural characterisation of **1** in the solid-state

The crystal used for data collection was crystallised from CH_2Cl_2 by slow evaporation although we found crystallisation was possible from a wide range of different solvents and solvent combinations. Data collection was performed with the aid of an Oxford Diffraction KM4 Sapphire CCD and a 4-circle kappa goniometer at 140 K. Cell refinement and data reduction were carried out with CRYSTALIS RED, release 1.6.9 β [27]. Data were corrected for absorption using the DELABS algorithm [28]. Structure solution, structure refinement, molecular graphics and geometrical calculations were performed with the SHELXTL software package [29]. The structure was refined using the full-matrix least-squares on F^2 with all non-H atoms anisotropically defined. H atoms were placed in calculated positions using the ‘riding model’ with $U_{\text{iso}} = a^* U_{\text{eq}}(\text{C})$ (where a is 1.5 for CH_3 groups and 1.2 for others). The 1.5 independent molecules show some disorder problems: the independent molecule, which does not lie on a twofold axis, shows two different dispositions. As the occupancy factor calculated for site A is close to 1 [0.909(3)] it was impossible to obtain both dispositions except for the metal ions and for two of the four chlorines. In order to obtain reasonable geometrical and displacement parameters, constraints (card AFIX 66 and EADP) and rigid body restraints (card DELU) were employed in the final stages of refinement.

3.7. Antimicrobial assays

The antimicrobial activity of the compounds was tested against the following:

Bacteria: *E. coli*. (G-ve ATCC 25922), *B. subtilis*. (G+ve ATCC 19659) and *P. aeruginosa*. (G-ve ATCC 27853). Fungi: *C. albicans* (ATCC 14053), *T. mentagrophytes* (ATCC 28185) and *C. resinae*.

The microbes were mixed at known concentrations with Mueller Hinton or Potato dextrose agar and poured into petri dishes so that after incubation a 'lawn' of microbial growth was observed. The compound to be tested is pipetted onto sterile filter paper disks and the solvent evaporated before being placed on the plates and incubated at 37 °C. For the compounds that are effective against the microbes, the size of the zones of growth inhibition around the disks was measured in mm (from the edge of the disk to the edge of the inhibition zone), with the antimicrobial activity being directly correlated to the size of the zone.

3.8. Antiviral assays

Samples of interest were pipetted onto 6 mm diameter filter paper disks and their solvents evaporated. The disks were placed directly onto BSC-1 cells (African Green Monkey kidney cells ATCC CCL 26), infected with either Herpes simplex type 1 virus (ATCC VR 733) or Polio virus type 1 (Pfizer vaccine strain), then incubated at 37 °C. Assays are examined after 24 h, using an inverted microscope, for the size of antiviral (i.e. viral inhibition) and or cytotoxic zones, and the type of cytotoxicity.

3.9. DNA binding assays

In this assay the complex (2.5 mM in 10 mM phosphate buffer, pH 7.2), was incubated for 4 h with 0.05 mg ml⁻¹ pBR322 DNA. The DNA damage was assessed by comparing the electrophoretic migration of the species in a 1% agarose gel, prepared in TAE buffer (40 mM Tris(hydroxymethyl)aminomethane acetate and 1 mM EDTA). From each assay, 8 µl were mixed with 1 µl dye (0.025 mg bromophenol blue, 1 ml glycerol and 1 ml distilled water) and pipetted into wells on the horizontal gel. A potential difference of 30 mV was applied over the gel for 4 h and the bands visualised by staining with ethidium bromide.

3.10. Laser ablation inductively coupled mass spectrometry study

Suspensions of *E. coli* JM109 (Promega, USA) in nutrient broth were incubated for 30 min at 37 °C with 5 (10 mM). The cells were pelleted by centrifugation and resuspended in distilled water (500 µl) and then sonicated. The cell debris was pelleted by centrifugation and the proteins in the supernatant fractions were separated by non-reducing SDS gel electrophoresis in a 10% polyacrylamide gel and visualised with coomassie brilliant blue G stain (Sigma). The gel was dried in cellulose membranes, placed on a Cetac LSX-200 Laser Ablation System (Cetac Technologies), which was coupled to a

Micromass Platform ICP Life-MS (Micromass UK Ltd). The gels were ablated using the laser and the resulting plasma analysed for the ruthenium isotopes using the Platform ICP.

4. Supplementary material

Crystallographic data are in cif format. Crystallographic data for the structural analysis have been deposited with the Cambridge Crystallographic Data Centre, CCDC no. 192375 for compound 1. Copies of this information may be obtained free of charge from The Director, CCDC, 12 Union Road, Cambridge CB2 1EZ, UK (Fax: +44-1223-336033; e-mail: deposit@ccdc.cam.ac.uk or www: <http://www.ccdc.cam.ac.uk>).

Acknowledgements

We would like to thank the Royal Society for a University Research Fellowship (P.J.D.), the University of York for a studentship (D.J.E.) and the EPFL for financial support.

References

- [1] B. Rosenberg, L. VanCamp, T. Krigas, *Nature* 205 (1965) 698.
- [2] G. Sava, R. Gagliardi, M. Cocchietto, K. Clerici, I. Marrella, E. Alessio, G. Mestroni, R. Milanino, *Pathol. Oncol. Res.* 4 (1998) 30.
- [3] P. Kopf Maier, H. Kopf, *Chem. Rev.* 87 (1987) 1137.
- [4] M.J. Clarke, F.C. Zhu, D.R. Frasca, *Chem. Rev.* 99 (1999) 2511.
- [5] G. Sava, A. Bergamo, *Int. J. Oncol.* 17 (2000) 353.
- [6] W.S. Sheldrick, S. Heeb, *Inorg. Chim. Acta* 168 (1990) 93.
- [7] (a) W.S. Sheldrick, H.S. Hagen-Eckhard, S. Heeb, *Inorg. Chim. Acta* 206 (1993) 15;
(b) S. Korn, W.S. Sheldrick, *Inorg. Chim. Acta* 254 (1997) 85;
(c) S. Korn, W.S. Sheldrick, *J. Chem. Soc. Dalton Trans.* (1997) 2191;
(d) P. Annen, S. Schildberg, W.S. Sheldrick, *Inorg. Chim. Acta* 307 (2000) 115.
- [8] (a) C.S. Allardyce, P.J. Dyson, D.J. Ellis, S.L. Heath, *Chem. Commun.* (2001) 1396;
(b) R.E. Morris, R.E. Aird, P.D. Murdoch, H.M. Chen, J. Cummings, N.D. Hughes, S. Parsons, A. Parkin, G. Boyd, D.I. Jodrell, P.J. Sadler, *J. Med. Chem.* 44 (2001) 3621.
- [9] (a) H.M. Chen, J.A. Parkinson, S. Parsons, R.A. Coxall, R.O. Gould, P.J. Sadler, *J. Am. Chem. Soc.* 124 (2002) 3064;
(b) F. Wand, H.M. Chen, J.A. Parkinson, P.D. Murdoch, P.J. Sadler, *Inorg. Chem.* 41 (2002) 4509.
- [10] D.S. Dwyer, K. Gordon, B. Jones, *Int. J. Immunopharm* 17 (1995) 931.
- [11] (a) T.W. Hayton, P. Legzdins, W.B. Sharp, *Chem. Rev.* 102 (2002) 935;
(b) N.A. Davies, M.T. Wilson, E. Slade, S.P. Fricker, B.A. Murrer, N.A. Powell, G.R. Henderson, *Chem. Commun.* (1997) 47.
- [12] (a) B. Cetinkaya, E. Cetinkaya, H. Kucukbay, R. Durmaz, *Arzneimittel-Forschung/Drug Res.* 46 (1996) 821;

- (b) M. Sulu, H. Kucukbay, R. Durmaz, S. Gunal, *Arzneimittel-Forschung/Drug Res.* 48 (1998) 291.
- [13] R.A. Sanchez-Delgado, M. Navarro, H. Perez, J.A. Urbina, *J. Med. Chem.* 39 (1996) 1095.
- [14] Shailendra, N. Bharti, M.T.G. Garza, D.E. Cruz-Vega, J.C. Garza, K. Saleem, F. Naqvi, A. Azam, *Bioorg. Med. Chem. Lett.* 11 (2001) 2675.
- [15] (a) R.A. Zelonka, M.C. Baird, *Can. J. Chem.* 50 (1972) 3063;
(b) C.W. Allen, K. Ramachandran, D.E. Brown, *Inorg. Synth.* 25 (1982) 74;
(c) M.A. Bennett, A.K. Smith, *J. Chem. Soc. Dalton Trans.* (1974) 233;
(d) G. Winkhaus, H. Singer, *J. Organomet. Chem.* 7 (1967) 487.
- [16] For example, see: (a) I. Moldes, E. de la Encarnación, J. Ros, Á. Alvarez-Larena, J.F. Piniella, *J. Organomet. Chem.* 566 (1998) 165;
(b) R. Bhalla, C.J. Boxwell, S.B. Duckett, P.J. Dyson, D.G. Humphrey, J.W. Steed, P. Suman, *Organometallics* 21 (2002) 924.
- [17] J.A. Cabeza, A. Nutton, B.E. Mann, C. Brevard, P.M. Maitlis, *Inorg. Chim. Acta* 115 (1986) L47.
- [18] W. Henderson, J.S. McIndoe, B.K. Nicholson, P.J. Dyson, *J. Chem. Soc. Dalton Trans.* (1998) 519.
- [19] P.J. Dyson, D.J. Ellis, D.G. Parker, T. Welton, *Chem. Commun.* (1999) 25.
- [20] G. Meister, G. Rheinwald, H. Stoeckli-Evans, G. Süß-Fink, *J. Chem. Soc. Dalton Trans.* (1994) 3215.
- [21] Y.N.V. Gopal, D. Jayaraju, A.K. Kondapi, *Biochemistry* 38 (1999) 4382.
- [22] C.S. Allardyce, P.J. Dyson, F.R. Abou-Shakra, H. Birtwhistle, J. Coffey, *Chem. Commun.* 1 (2001) 2708.
- [23] C.S. Allardyce, P.J. Dyson, *J. Cluster Sci.* 12 (2001) 563.
- [24] D.F. Baban, L.W. Seymour, *Adv. Drug Delivery Rev.* 34 (1998) 109.
- [25] H.Z. Sun, H.Y. Li, P.J. Sadler, *Chem. Rev.* 99 (1999) 2817 (and references cited therein).
- [26] M.J. Clarke, in: M.J. Clarke (Ed.), *Progress in Clinical Biochemistry and Medicine*, Springer-Verlag, Berlin, 1989, pp. 25–39.
- [27] Oxford Diffraction Ltd, Abingdon, Oxfordshire, UK, 2001.
- [28] Walker, N., Stuart, D. *Acta Crystallogr. Sect. A* 39 (1983) 158–166.
- [29] G.M. Sheldrick, University of Göttingen, Germany, 1997; Bruker AXS Inc., Madison, WI, USA, 1997.